

Improved Sunflower Optimization Algorithm Tuned Adaptive Type-2 Fuzzy PID Controller for Frequency Regulation of Renewable Power Integrated Hybrid Distributed Power System

Smrutiranjana Nayak*, Sanjeeb Kumar Kar***, Subhransu Sekhar Dash***

*Department of Electrical Engineering, ITER, Siksha 'O' Anusandhan University, Odisha, India

** Department of Electrical Engineering, ITER, Siksha 'O' Anusandhan University, Odisha, India

*** Department of Electrical Engineering, Government College of Engineering, Keonjhar, Odisha, India

(smrutikiit40@gmail.com, sanjeebkar@soa.ac.in, subhransudash_fee@gcekjr.ac.in)

Corresponding author: Subhransu Sekhar Dash

Received: 30.08.2021 Accepted: 11.10.2021

Abstract- The indeterminate characteristic of renewable sources makes present power systems very complex and introduces the frequency fluctuations. This work proposes a maiden application of an Improved Sunflower Optimization Algorithm (ISFO) technique tuned Adaptive Type-2 Fuzzy PID (AT2FPID) controller for frequency control of hybrid distributed power systems integrated with renewable sources. Initially, PID controller are considered and the dominance of ISFO over Sunflower Optimization Algorithm (SFO), Genetic Algorithm (GA) and Differential Evolution (DE) has been established. Performance comparison is carried out by assessing overshoots, undershoots and various integral errors due to Step Load Perturbations (SLPs) in each area. In the next stage, AT2FPID controller is considered and its supremacy to control the system frequency is demonstrated by comparing with Type-2 Fuzzy PID (T2FPID), Type-1 Fuzzy PID (T1FPID) and PID controllers for various cases.

Keywords- Sunflower Optimization Algorithm (SFO), Improved SFO (ISFO), Distributed Energy Sources, renewable sources, Frequency Control, Adaptive Type-2 Fuzzy PID (AT2FPID) Controller.

1. Introduction

The integration of solar and wind sources to the grid, though decreases the dependency on fuel-based energy sources, introduces generation load mismatch and hence frequency variation of 50 hertz. Load Frequency Controllers (LFC) are provided to regulate the frequency variations within the limits [1]. Various schemes have been presented in the literature for LFC [2-5]. In most cases, conventional power systems are considered but very few cases address the LFC in presence of distributed and renewable sources. This study suggests an LFC scheme for power systems when integrated with distributed and renewable sources.

Conventional PID controllers are unable to deliver the required performance if nonlinearity and constraints are present in the system [6-8]. A Fuzzy Logic Controller (FLC) can deal with nonlinearity and uncertainty. Various fuzzy-

based LFC schemes such as hPSO-PS tuned FLC [6], ICA tuned Fractional Ordered (FO) Fuzzy PID (FPID) [7] and BFOA tuned FOFPID [8]. When large uncertainties are present, the conventional fuzzy structure may not be effective and the controller structure can be modified to make it adaptive as proposed. The dual membership function-based Type-2 FPID (T2FPID) controllers, alternatively, give a better dynamic performance in this case [9]. This paper proposes an Adaptive Type-2 FPID (AT2FPID) structure to improve the performance of T2FPID [10].

Literature study shows that, various techniques are employed to design controllers for AGC. The techniques include Differential evolution (DE)[11, 12], Particle swarm optimization (PSO)[13, 14], Artificial bee colony (ABC) [15], Cuckoo search (CS) [16], Teaching Learning Based Optimization (TLBO) [17], Adaptive neuro fuzzy

interference system (ANFIS) [18], Bat algorithm [19], Grey Wolf Optimization (GWO) [20, 21] etc. Conferring to ‘No Free Lunch theorem (NFL)’, there is no method existing for all kinds of problems. Sunflower Optimization Algorithm (SFO) is a newly projected optimization approach encouraged by the orientation of sunflowers towards sun light [22]. It is enthused by the “inverse-square law of radiation intensity,” where the strength of solar energy (i.e., heat) is directly related to the squared distance between the flowers and the sun. It is based on the positioning of flowers, which models the cross-pollination formed among arbitrary adjacent flowers to attain the optimum position/solution. In the initial periods of SFO algorithm, the best position is unidentified. The SFO is a new meta-heuristic algorithm which is stimulated by the moving of sunflowers towards the sunlight by considering the pollination between adjacent sunflowers. Thus, big initial steps may move the solutions away from optimum position. Consequently, scaling factors can be employed to modify the positions in the initial phases in the proposed Improved SFO (ISFO) which is employed to tune the controller parameters.

The objectives of this study are:

- An AT2FPID structure is suggested for frequency control of power system with distributed and renewable sources.
- A Sine Cosine adopted Improved SFO (ISFO) algorithm is developed by using Sine Cosine adopted scaling factor in SFO technique.
- The impact of ISFO based AT2FPID for frequency regulation in the studied system is examined and is compared with T2FPID, T1FPID and PID for different cases.
- Real time validation is done by comparing the results with OPAL-RT results.

2. Investigated System

Fig.1 displays the studied power system with distributed and renewable sources. It contains thermal power system and DG units like FC (Fuel-cell), HAE (Hydro-Aqua Electrolysers), MTG (Micro Turbine), BESS (Battery Energy Storage System) and DEG (Diesel Engine Generator) [2, 23-24]. It also contains solar and wind-based plants one in each area. The nominal parameters are taken from ref. [2, 23-24].

2.1. Mathematical Modeling of Components

2.1.1 Wind turbine generator (WTG):

The wind turbine power is described by wind velocity V_w and power coefficient C_p as:

$$P_{WP} = \frac{1}{2} \rho A_r C_p V_w^3 \tag{1}$$

where ρ is air density and A_r is swept area of blades. The transfer function (TF) model for small signal studies is given by [13]:

$$G_{WTG}(s) = \frac{K_{WTG}}{1 + sT_{WTG}} \tag{2}$$

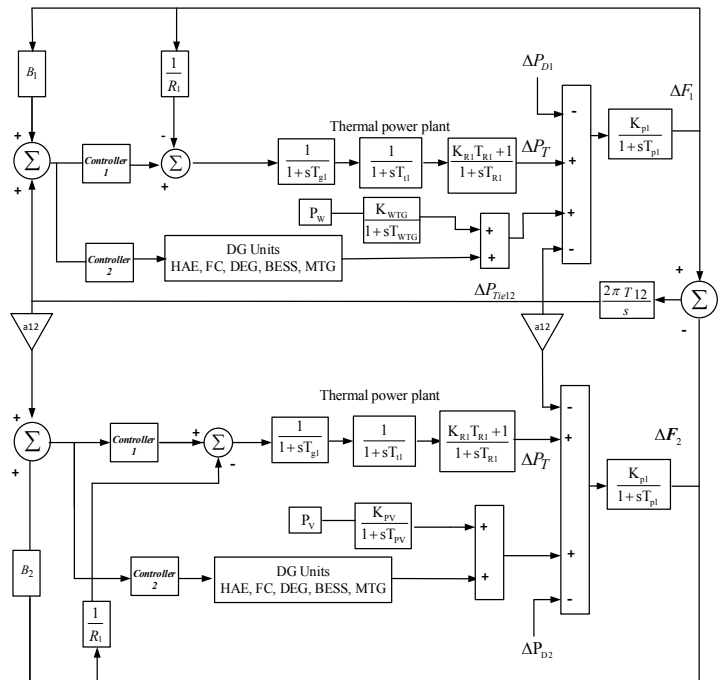


Fig. 1. Investigated hybrid multi-area system

2.1.2 Solar PV Modelling:

The PV power output is given by [1]:

$$P_{pv} = \eta S \gamma [1 - 0.005 (T + 25)], \tag{3}$$

Where, η = PV cell conversion efficiency with a value of 10%, S = PV array area with a value of 4084m²
 ϕ = solar irradiation in kW/m², T_a = ambient temperature in degree Celsius ($T = 25^\circ\text{C}$).

First order transfer function of this system during low frequency domain analysis is given by

$$G_{PV}(s) = \frac{K_{PV}}{1 + sT_{PV}} = \frac{\Delta P_{PV}}{\Delta \phi} \tag{4}$$

2.1.3 DG Units Modelling:

The TF representation of HAE (Hybrid-Aqua Electrolyser), FC (Fuel cell), DEG (Diesel Engine Generator), BESS (Battery Energy Storage System) and MTG (Microturbine Generation) are given by [24]:

$$G_{HAE}(s) = \frac{K_{HAE}}{1 + sT_{HAE}} \tag{5}$$

$$G_{FC}(s) = \frac{K_{FC}}{1 + sT_{FC}} \tag{6}$$

$$G_{DEG}(s) = \frac{K_{DEG}}{1 + sT_{DEG}} \quad (7)$$

$$G_{BESS}(s) = \frac{K_{BESS}}{1 + sT_{BESS}} \quad (8)$$

$$G_{MTG}(s) = \frac{K_{MTG}}{1 + sT_{MTG}} \quad (9)$$

2.1.4 Thermal power plant:

The thermal power system contains generator, turbine, governor and reheater with TFs[7]:

$$G_p(s) = \frac{K_p}{1 + sT_p} \quad (10)$$

$$G_t(s) = \frac{K_t}{1 + sT_t} \quad (11)$$

$$G_g(s) = \frac{K_g}{1 + sT_g} \quad (12)$$

$$G_r(s) = \frac{1 + sK_rT_r}{1 + sT_r} \quad (13)$$

2.1.5 Power system and load:

The TF of the power system and load is represented by [1]:

$$G_p(s) = \frac{K_p}{1 + sT_p} \quad (14)$$

3. Suggested Approach

3.1. AT2FPID controller structure

Type-2 fuzzy sets are an extension to type-1 fuzzy sets with twin membership function (MF). The association of the Upper MF (UMF) and the Lower MF (LMF) structures the MFs of type-2 fuzzy controllers. To control the overall membership mechanism of each linguistic variable, there could be two separate membership values at the root, namely LMF and UMF. Fuzzification is the fuzzy controller's key operation. From different membership features, the fuzzification method accesses all inputs (*e*, *de*) and generates sensible 3-dimension ordered fuzzy sets. An Adaptive Type-2 Fuzzy PID (AT2FPID) structure is proposed in this work in which the input signal is passed through Type-2 fuzzy as well as PID. The structure of AT2FPID employed is revealed in Fig. 2. The membership-functions-of-AT2FPID-structure contains 3 MFs for inputs/output. The following parameters are used for the 3 MFs: $\mu_1 = -1$, $\mu_2 = 0$, $\mu_3 = 1$, $\Delta\mu = 1/8$,

and $\sigma = 0.418$), the course UMF is Gaussian with $\mu = 0$, and $\sigma = 0.5128$, the LMF is a trimmed Gaussian, with $\mu = 0$, 0.3532, and a scaling variable of 0.895.

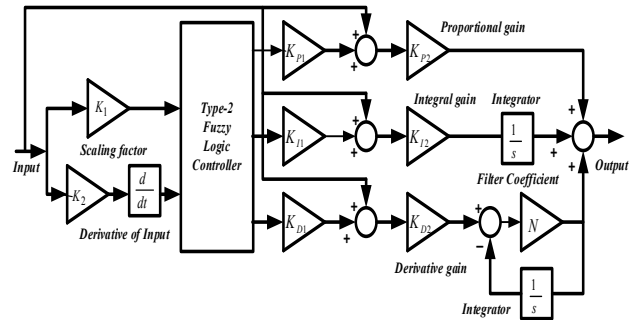


Fig.2. AT2FPID controller structure

3.2. Objective function

An integral measure that minimizes both frequency & tie-line power variations and control efforts, is employed as:

$$J = \int_0^t [k_n w \{ \sum (\Delta f_i)^2 + (\Delta P_{Tie})^2 \} + (1-w) \{ \sum (\Delta U_i)^2 \}] dt \quad (15)$$

Where *t* is the time, Δf_i and ΔP_{Tie} are the deviations in frequency and line power, ΔU_i 's are the controller outputs. To make the both components in Eq. (15) participate in the optimization, k_n and w are allotted values of 1000 and 0.5. The constraints are:

$$\begin{aligned} K_{P_{i\min}} &\leq K_{P_i} \leq K_{P_{i\max}}, K_{I_{i\min}} \leq K_{I_i} \leq K_{I_{i\max}}, \\ K_{D_{i\min}} &\leq K_{D_i} \leq K_{D_{i\max}} \\ K_{1\min} &\leq K_1 \leq K_{1\max}, K_{2\min} \leq K_2 \leq K_{2\max} \end{aligned} \quad (16)$$

Where the subscripts 'min' and 'max' represent the limiting values.

4. Improved Sun Flower Optimization (ISFO) Algorithm

The sunflower optimization technique is a high random element-based biological behaviour-inspired tuning technique that was projected in [10]. This tuning technique is inspired by the biological characteristic of the sunflowers, its face movement automatically towards the sun. During this type of orientation of flower facing towards the sun position, the impregnation may have ensued between the nearby adjacent sunflowers [25-31]. For individual sunflowers, the cumulative captivated contamination is based on the length between it and the sun. The net reduction of absorbed energy between the sunflowers & the sun for each decaying length between them is as the following equation.

$$I = \frac{P_s}{4\pi d^2} \quad (17)$$

Where I am the strength of the solar irradiance, P_s is the solar power and d is the length among individual sunflower & the sun [11]

4.1. Sunflower path directives

Individually sunflower fine-tunes its orientation towards the sun as given in the equation below:

$$S_i = \frac{X^* - X_i}{|X^* - X_i|}; i = 1, 2, 3 \dots n \tag{18}$$

X^* is the optimal solution, X_i is the present solution and n is the size of the population.

The step size of each sunflower along the sun is characterized as below:

$$d_i = \alpha * P_i(|X_i + X_{i-1}| * |X_i + X_{i-1}|) \tag{19}$$

α is the flower’s inertial shift, $P_i(|X_i + X_{i-1}|)$ is the possibility of the fertilization that each flower can pollinate the nearby flower to shift the new sunflowers in a novel location based on the gap among them.

Individual sunflower stage is limited not to be more than the following boundary value

$$d_{max} = \frac{|X_{max} - X_{min}|}{2 * n} \tag{20}$$

Where X_{max} , X_{min} are the upper and lower limits respectively and ‘ n ’ denotes the population size.

4.2. Upgradation of sunflower location

Individual sunflower, i updates its position to form a fresh group of sunflowers depending on the orientation and the stage of sunflowers along with the sun as follows.

$$X_{i+1} = X_i + d_i * s_i \tag{21}$$

Where X_{i+1} is the new location due to freshly generated sunflower.

In the initial periods of SFO algorithm, the best position is unidentified. Thus, big initial steps may move the solutions away from optimum position. Consequently, scaling factors can be employed to modify the positions in the initial phases in the proposed Improved SFO (ISFO) which is employed to optimize controller values.

In proposed ISFO, individual sunflower, i updates its position as follows.

$$X_{i+1} = (X_i + d_i * s_i) / SF \tag{22}$$

Where SF is the sine cosine adapted scaling factors which are calculated as:

$$SF = \begin{cases} W * \sin\left(\pi * \left(\frac{it}{IT}\right)\right) & \text{if } RND1 < 0.5 \\ W * \cos\left(\pi * \left(\frac{it}{IT}\right)\right) & \text{if } RND1 \geq 0.5 \end{cases} \tag{23}$$

For the appropriate selection of W , various W values are tried and it is seen that the finest outcomes are found when W

is selected as 100. The cyclic function pattern of sine and cosine functions allow a result to be relocated around alternative result. This process can guarantee better exploitation and exploration capability of algorithm. The flow-chart of SFO is shown in Fig.3.

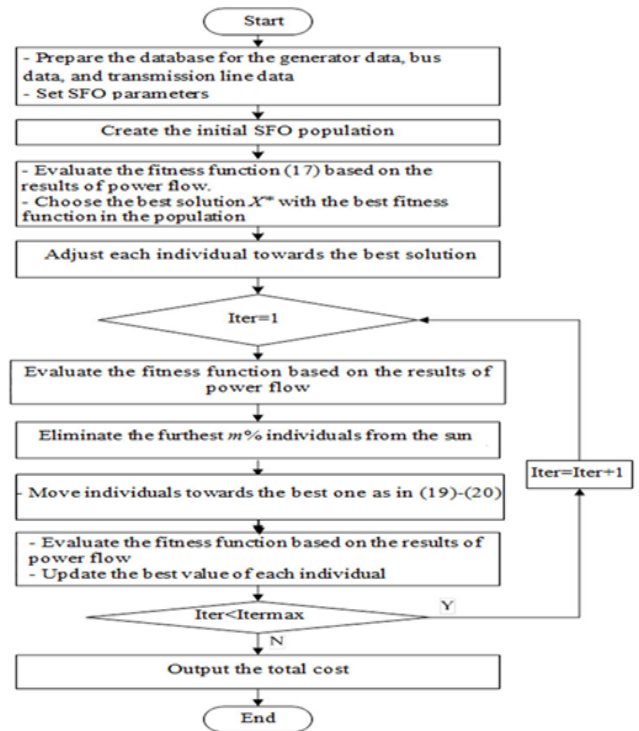


Fig.3. Flow chart of SFO

5. Results and discussion

Proposed ISFO is now applied to design AT2FPID controllers for the system shown in Fig.1. A 5% step load disturbance in area-1 and 3% SLP in area-2 is applied. The system's frequency gets influenced by the load disturbances which is regulated by the controllers. To authenticate the dominance of ISFO, firstly PID structures are considered and the controller are optimized by ISFO, SFO, DE and GA methods. The algorithms parameters are taken from reference [3, 23]. The range of parameters is selected to be [0, 2]. For all the algorithms, search agents and iterations are selected as 30 and 100 and run 30 times. The optimized values are gathered in Table1 from which it is obvious that minimum J value is attained with ISFO compared to GA, DE and SFO. The %reduction in J value with ISFO method correlated to GA, DE and SFO are 59.36%, 32.11% and 17.46% respectively. The frequency deviation of area-1 for the above condition is revealed in Fig.4 from which it is obvious that, the performance with ISFO method is better than GA, DE and SFO techniques. The numerical comparison using various integral errors, maximum overshoot (MOs) and maximum undershoot (MUs), of ΔF_1 , ΔF_2 , of the proposed system for above case are collected in Table 2 from which it is seen that the results with ISFO optimized PID are less in almost all the cases compared same with GA, DE and SFO.

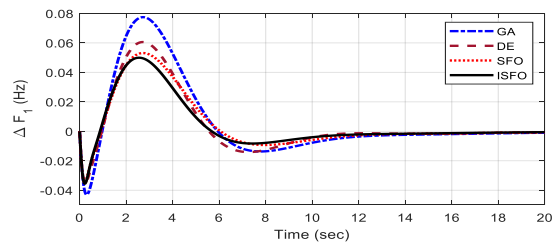


Fig.4. Comparison of techniques

Table 1. Optimal PID controller parameters

Technique/ Controller	Controller-1			Controller-2			J Value
	K_P	K_I	K_D	K_P	K_I	K_D	
GA	1.0158	1.1385	1.1234	0.0015	0.0011	0.0021	14.2146
DE	1.3178	1.64485	1.7386	0.0664	0.0105	0.0108	8.5086
SFO	1.7513	1.5887	1.9513	1.7446	0.0814	1.8233	6.9976
ISFO	1.8781	1.8661	1.8581	0.0018	0.0395	1.8261	5.7757

Table 2. Performance index comparison of different techniques

Controller/ Technique	Integral errors					MOs		MU _s (-ve)	
	ISE	ITAE	ITSE	IAE	ISTAE	ΔF_1	ΔF_2	ΔF_1	ΔF_2
GA	0.0281	3.2459	0.0908	0.6657	27.7174	0.0775	0.0739	0.0430	0.0294
DE	0.0167	2.3959	0.0538	0.5079	19.4259	0.0606	0.0573	0.0351	0.0233
SFO	0.0137	2.3199	0.0443	0.4706	20.0470	0.0531	0.0503	0.0351	0.0228
ISFO	0.0112	1.9393	0.0337	0.4140	16.4633	0.0499	0.0468	0.0355	0.0231

Table 3. ISFO optimized controller parameters

Technique/ Controller	Controller-1					Controller-2					J Value
	K_I	K_2	K_P	K_I	K_D	K_I	K_2	K_P	K_I	K_D	
T1FPID	1.8607	1.8558	1.5942	1.7774	0.0787	1.2020	0.2365	0.0053	0.2202	0.0009	2.1801
T2FPID	1.8779	1.8731	1.7957	1.7209	0.3463	0.3007	0.1591	0.1829	0.0017	0.0018	0.3783
AT2FPID	1.7985	1.7998	1.9081	1.9085	1.7982	1.4967	0.0285	1.5892	0.1698	1.8853	0.2281
			1.7989	1.8687	0.3791			1.9002	1.8802	0.0398	

In the next step, T1FPID, T2FPID and AT2FPID controllers are tuned by ISFO technique. The tuned controller values are specified in Table 3 from which it is obvious that, reduced J value is obtained with AT2FPID related to T2FPID and T1FPID. The % reduction in J value with AT2FPID related to PID, T1FID and T2FPID are 96.05%, 89.53% and 39.71% respectively.

To compare the performance, different cases (other than the conditions at which the controllers are designed) are considered.

Case 1: SLPs in each area without the considering solar/wind sources disturbances.

Case 2: Variation in SLPs with the change in wind speed with no variation in sun irradiance.

Case 3: Variation in SLPs with the variations in solar and wind sources.

Case 4: Increased solar and wind power integration.

Case 5: Unavailability of solar and wind powers.

Case 6: Variation in system parameters.

Case 1:

In this case, a 5% SLP in area-1 ($P_{D1}=0.05$), 3% SLP in area-1 ($P_{D2}=0.03$) in area-2, wind power $P_{WTG}= 0.124$ p.u. (wind speed =9 m/s) and solar power of 0.153 p.u. is considered. These variations are displayed in Fig.5(a). The responses with ISFO optimized AT2FPID, T2FPID, T1FPID and PID are revealed in Figs.5(b)-(d). The assessment report of transient characteristics is given in Table-4. It can be noticed from Figs.5(b)-(d) and Table-4 that, the transient performance with ISFO optimized

AT2FPID is superior than PID, T1FPID and T2FPID controllers with respect to low errors and MUs/MOs in contrast to other controllers. The % decrease in J value with AT2FPID related to T2FPID, T1FPID and PID controller are 39.74%, 89.55%, and 96.05% respectively.

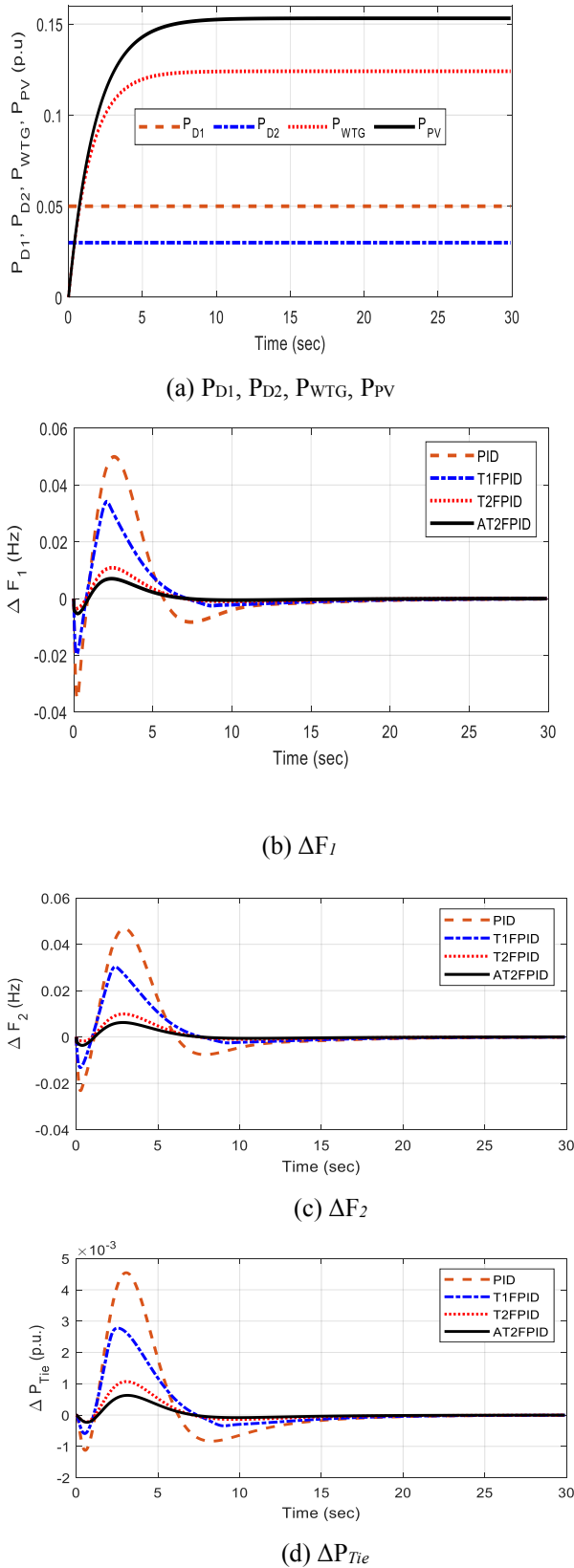


Fig.5. System response for Case-1

Case 2:

In this case, SLPs of area-1 and 2 are increased by 2% and wind speed (V_w) is decreased by 2 m/s at $t=30$ s compared to Case-1. These variations are shown in Fig.6 (a). The dynamic response with ISFO optimized AT2FPID, T2FPID, T1FPID and PID are revealed in Figs.6(b)-(d). The assessment report of transient characteristics is given in Table-5. It can be noticed from Figs.6(b)-(d) and Table-5 that, the system performance with ISFO optimized AT2FPID is better than PID, T1FPID and T2FPID controllers. In this case, the % reduction in J value with AT2FPID related to T2FPID, T1FPID and PID controller are 42.21%, 89.79%, and 96.13% respectively.

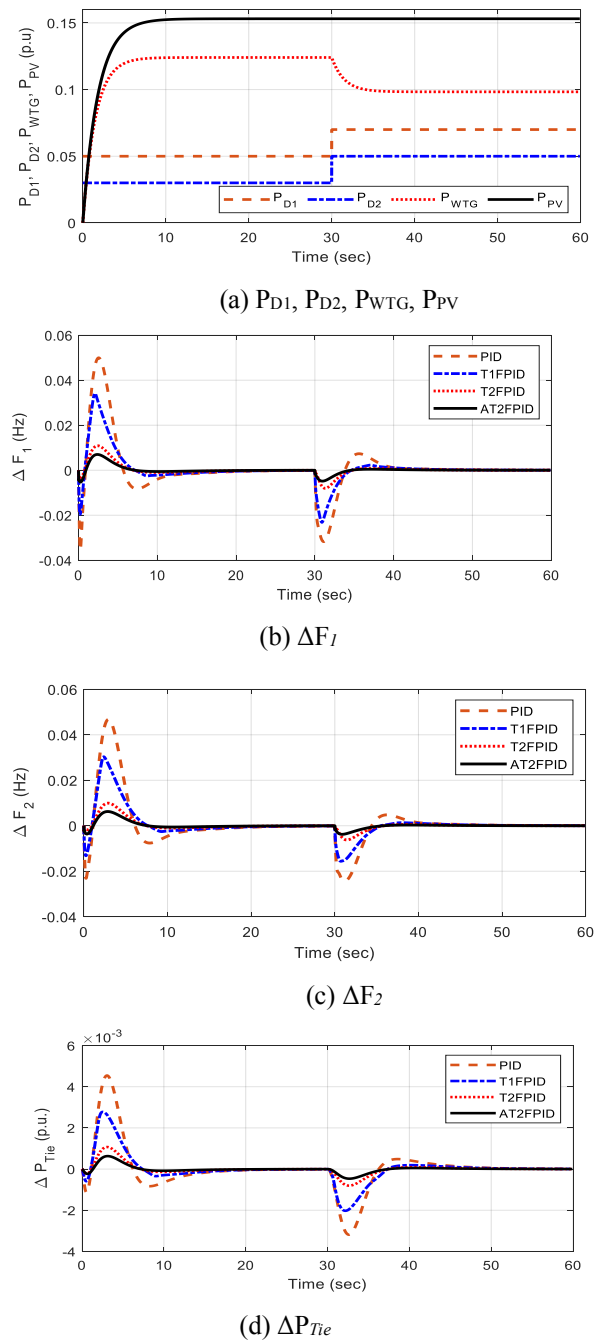


Fig.6. System response for Case-2

Table 4. Performance index comparison of ISFO optimized controllers for Case-1

Controller/ Technique	J value	Integral errors					MO _s		MU _s (-ve)	
		ISE	ITAE	ITSE	IAE	ISTAE	ΔF ₁	ΔF ₂	ΔF ₁	ΔF ₂
PID	5.7753	0.0112	1.9388	0.0337	0.414	16.4472	0.0499	0.0468	0.0355	0.0231
T1FPID	2.1797	0.0041	1.1348	0.0115	0.2456	10.2207	0.0341	0.0303	0.0196	0
T2FPID	0.3779	5.3813e-04	0.4982	0.0017	0.0936	4.8882	0.0109	0.0099	0.0045	0.0023
AT2FPID	0.2277	2.3495e-04	0.3068	6.9286e-04	0.0621	2.9555	0.0070	0.0062	0.0053	0.0036

Table 5. Performance index comparison of ISFO optimized controllers for Case-2

Controller/ Technique	J value	Integral errors					MO _s		MU _s (-ve)	
		ISE	ITAE	ITSE	IAE	ISTAE	ΔF ₁	ΔF ₂	ΔF ₁	ΔF ₂
PID	7.4822	0.0146	9.0991	0.1409	0.6266	261.0749	0.0499	0.0468	0.0355	0.0244
T1FPID	2.8327	0.0054	5.2623	0.0511	0.3683	151.4661	0.0341	0.0303	0.0231	0
T2FPID	0.5005	7.3304e-04	2.2399	0.0079	0.1446	65.4789	0.0109	0.0099	0.0080	0.0062
AT2FPID	0.2892	3.0645e-04	1.3463	0.0030	0.0927	38.9667	0.007	0.0062	0.0053	0.0038

Table 6. Performance index comparison of ISFO optimized controllers for Case-3

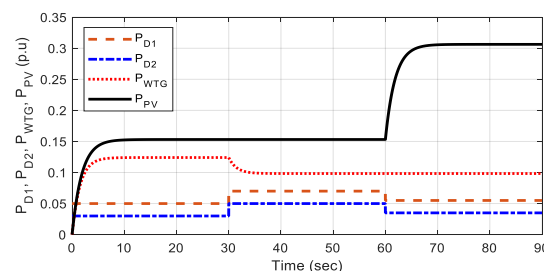
Controller/ Technique	J value	Integral errors					MO _s		MU _s (-ve)	
		ISE	ITAE	ITSE	IAE	ISTAE	ΔF ₁	ΔF ₂	ΔF ₁	ΔF ₂
PID	10.3223	0.0197	28.0323	0.4585	0.9200	1.4895e+03	0.0499	0.0468	0.0355	0.0244
T1FPID	4.1787	0.0077	17.4834	0.1910	0.5582	942.7179	0.0341	0.0314	0.0231	0.0023
T2FPID	0.9125	0.0011	7.5543	0.0328	0.2267	411.6659	0.0109	0.0112	0.0080	0.0062
AT2FPID	0.5726	4.4378e-04	4.5065	0.0115	0.1416	244.5423	0.0070	0.0064	0.0053	0.0038

Table 7. Performance index comparison of ISFO optimized controllers for Case-4

Controller/ Technique	J value	Integral errors					MO _s		MU _s (-ve)	
		ISE	ITAE	ITSE	IAE	ISTAE	ΔF ₁	ΔF ₂	ΔF ₁	ΔF ₂
PID	42.2258	0.0785	47.9482	1.2635	1.7472	2.5586e+03	0.1159	0.1073	0.0431	0.0297
T1FPID	18.3888	0.0326	30.2609	0.5446	1.0871	1.6345e+03	0.0840	0.0728	0.0322	0.0039
T2FPID	4.6076	0.0051	13.1891	0.0963	0.4562	717.9815	0.0282	0.0253	0.0111	0.0077
AT2FPID	2.9706	0.0018	7.7965	0.0328	0.2710	423.6572	0.0169	0.0151	0.0064	0.0042

Case 3:

In this case, SLPs of area-1 and 2 are decreased by 1.5% and sun radiation is increased by 0.15 p.u. at t=60 s compared to Case-2. These load and power variations are exposed in Fig.7(a). The dynamic responses are revealed in Figs.7(b)-(d). The comparison report of transient characteristics is given in Table-6. It can be noticed from Figs.7(b)-(d) and Table-6 that, the response with ISFO optimized AT2FPID is better than PID, T1FPID and T2FPID controllers. In this case, the % reduction in J value with AT2FPID related to T2FPID, T1FPID and PID controller are 37.24%, 86.29%, and 94.45% respectively.



(a) P_{D1}, P_{D2}, P_{WTG}, P_{PV}

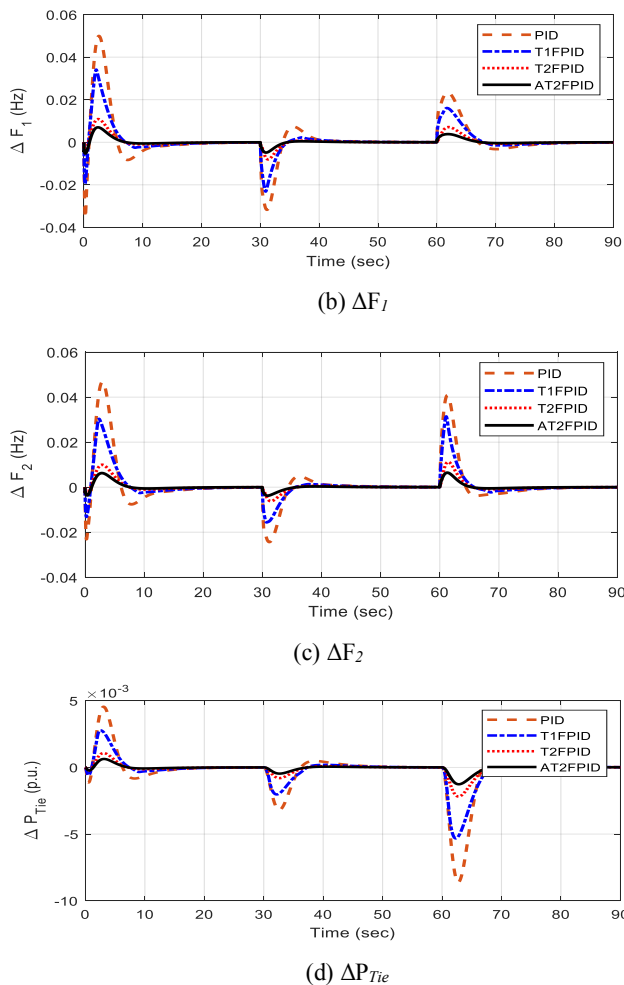
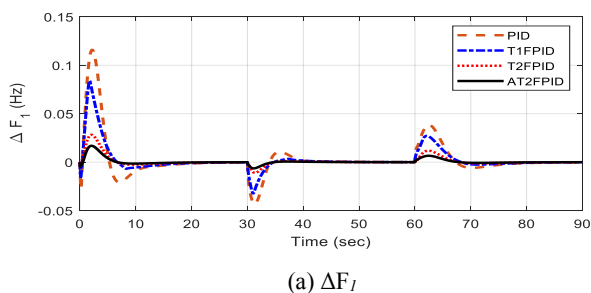


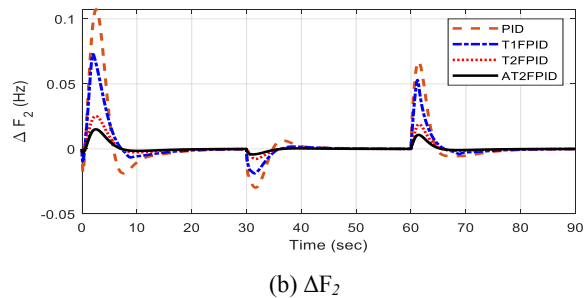
Fig.7. System response for Case-3

Case 4:

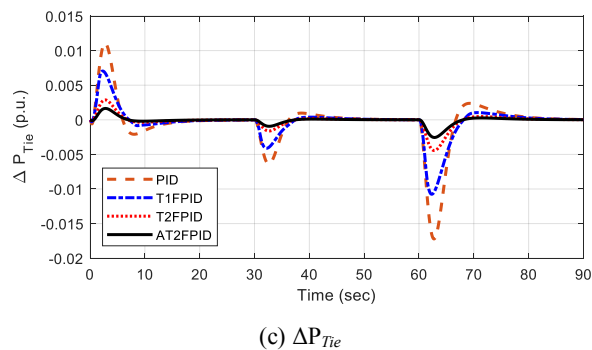
Here, the solar and wind powers integration is augmented by 100% compared to Case-3. The response for the above case is exposed in Fig. 8(a)-(c) and the numerical performances are gathered in Table 7. It can be observed that, in this case also, the response with suggested AT2FPID is superior to that with PID and FPID and T2FPID controllers. The % reduction in *J* value with AT2FPID related to T2FPID, T1FPID and PID controller are 35.52%, 83.84%, and 92.96% respectively for case-4.



(a) ΔF_1



(b) ΔF_2

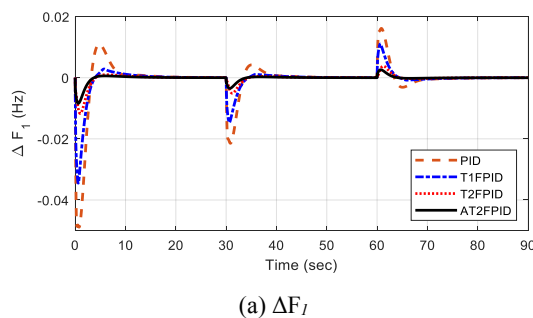


(c) ΔP_{Tie}

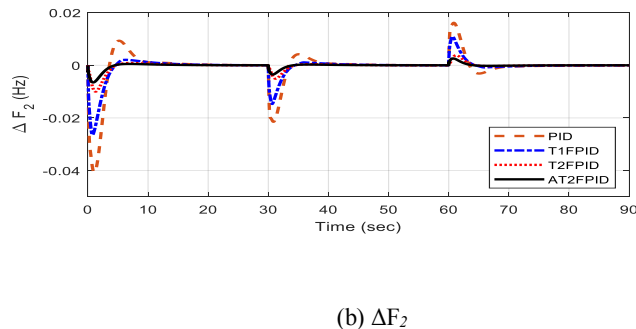
Fig.8. System response for Case-4

Case 5:

It is assumed that the renewables sources are not available but the load demands are varying as in Case 3. The response for the above case is revealed in Fig.9 (a)-(b) and the numerical performances are gathered in Table- 8. It can be observed that, the responses with recommended AT2FPID is better than PID and FPID and T2FPID controllers. The % reduction in *J* value with AT2FPID related to T2FPID, T1FPID and PID controller are 29.43%, 81.83%, and 93.22% respectively for case-5.



(a) ΔF_1



(b) ΔF_2

Fig.9. System response for Case-5

Table 8. Performance index comparison of ISFO optimized controllers for Case-5

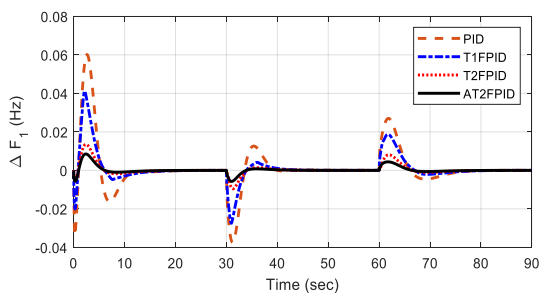
Controller/ Technique	J value	Integral errors					MOs		MU _s (-ve)	
		ISE	ITAE	ITSE	IAE	ISTA	ΔF ₁	ΔF ₂	ΔF ₁	ΔF ₂
PID	5.0572	0.0096	11.1800	0.1155	0.5035	532.9378	0.0161	0.0161	0.0489	0.0407
T1FPID	1.8852	0.0033	6.1034	0.0393	0.2736	292.1511	0.0110	0.0110	0.0345	8.1226e-04
T2FPID	0.4852	5.1305e-04	2.6181	0.0061	0.1161	125.3768	0.0038	0.0038	0.0117	0.0100
AT2FPID	0.3424	2.2112e-04	1.6192	0.0025	0.0727	77.5310	0.0026	0.0026	0.0084	0.0065

Table 9. Performance index comparison of ISFO optimized controllers for Case-6

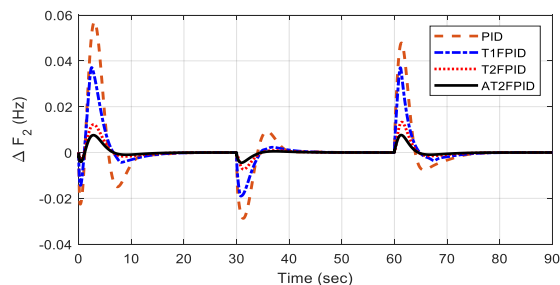
Controller/ Technique	J value	Integral errors					MOs		MU _s (-ve)	
		ISE	ITAE	ITSE	IAE	ISTA	ΔF ₁	ΔF ₂	ΔF ₁	ΔF ₂
-25%										
PID	14.1091	0.0273	30.9671	0.6109	1.0564	1.6126e+03	0.0602	0.0570	0.0374	0.0288
T1FPID	5.5145	0.0104	18.7492	0.2511	0.6178	995.1681	0.0412	0.0371	0.0274	0.0036
T2FPID	1.0806	0.0015	7.9541	0.0415	0.2475	427.2156	0.0135	0.0133	0.0096	0.0073
AT2FPID	0.6253	5.7628e-04	4.7480	0.0145	0.1538	254.1584	0.0085	0.0076	0.0057	0.0045
+25%										
PID	7.7908	0.0147	23.8089	0.3473	0.7717	1.2787e+03	0.0424	0.0392	0.0374	0.0242
T1FPID	3.1975	0.0057	15.1890	0.1428	0.4819	825.3013	0.0289	0.0270	0.0205	0.0012
T2FPID	0.7807	8.4734e-04	6.6419	0.0254	0.1965	364.2803	0.0089	0.0096	0.0068	0.0054
AT2FPID	0.5311	3.4135e-04	3.9617	0.0089	0.1238	216.1086	0.0059	0.0055	0.0052	0.0034

Case 6:

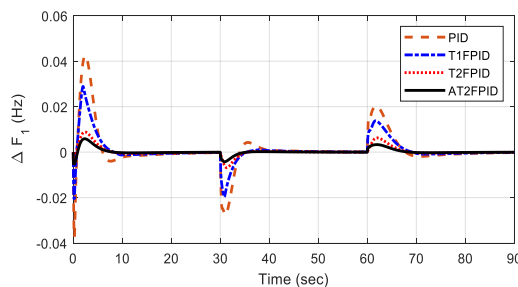
In real-world systems, it is likely to have an imprecision of parameters employed and they may change with time, affecting the performance. Therefore, it is essential to investigate the system performance under parameter variations. For this, the system parameter (gains and time constants of all components) is changed by ±25%. The evaluation description under the above varied cases is gathered in Table-9. The system response for the above case is exposed in Fig.10(a)-(d). It is clear from Table-9 and Fig.10 that projected scheme for frequency control is robust and achieves acceptable performance in presence of parameter uncertainty.



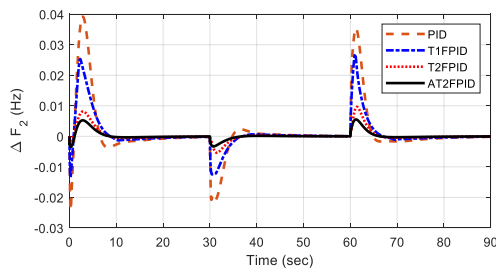
(a) ΔF₁ at -25%



(b) ΔF₂ at -25%



(c) ΔF₁ at +25%



(d) ΔF_2 at +25%

Fig.10. System response for Case-6



Fig.11 (a). OPAL-RT simulator setup

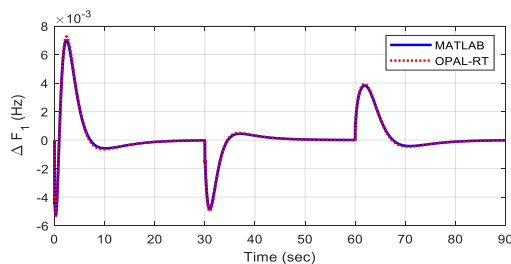


Fig.11(b). OPAL-RT Vs MATLAB results

Finally, to examine the real time application of projected scheme, MATLAB results are related to OPAL-RT results. The OPAL-RT set up is shown in Fig. 11 (a). In this case all variations as mentioned in Case-3 is considered. The comparative results are revealed in Fig. 11 (b) from which it is obvious that MATLAB/SIMULINK results are quite close to that of OPAL-RT results.

6. Conclusion

In this work, a Sine Cosine based Improved SFO (ISFO) for is suggested for an Adaptive Type-2 Fuzzy PID (AT2FPID) controller design for frequency control of a hybrid distributed multi-area power system. It is observed that with the same PID, better result is attained by ISFO related to SFO, DE and GA methods. The % reduction in *J* value with projected ISFO method related to GA, DE and SFO are 59.36%, 32.11% and 17.46% respectively. The performance of proposed frequency control approach is found to be effective with increase of wind, PV power as well as load demand changes. It is noticed that AT2FPID is superior than PID, T1FPID and T2FPID controllers for frequency regulation. It is noticed that the performance of

projected frequency control scheme is robust and effective under increased renewable penetration or unavailability of renewable sources as well as change in system parameters. The proposed sunflower optimization algorithm (SFO) technique is a population-based iterative heuristic global optimization algorithm for multi-modal problems. Compared to traditional algorithms, SFO employs terms as root velocity and pollination providing robustness. The new method is then applied in an inverse problem of structural damage detection in composite laminated plates.

To authenticate the viability of the approach, MATLAB results are equated with OPAL-RT results and it is observed that MATLAB/SIMULINK results are quite close to that of OPAL-RT results.

Acknowledgement:

This article is the modified & extended version of the paper titled "Frequency regulation of hybrid distributed power systems integrated with renewable sources by optimized type-2 fuzzy PID controller" presented in the 9th International Conference on SMART GRID (29 June-July 1, 2021 at Setubal/Portugal.-

References

- [1] Elgerd OI. Electric energy systems theory. Tata McGraw Hill, New Delhi 2006.
- [2] R.K. Khadanga, A. Kumar, S. Panda, "A novel modified whale optimization algorithm for load frequency controller design of a two-area power system composing of PV grid and thermal generator", *Neural Comput & Applications*, 32, 8205–8216, 2020.
- [3] B. Mohanty, S. Panda, P.K. Hota, "Controller parameters tuning of differential evolution algorithm and its application to load frequency control of multisource power system. *International Journal of Electrical Power Energy System*". 54,77-85,2014.
- [4] RK. Sahu, S. Panda, S. Padhan, "Optimal gravitational search algorithm for interconnected power systems", *Ain Shams Eng. J.*5, 721–733.2014
- [5] S. Panda, B. Mohanty, P.K. Hota, "Hybrid BFOA-PSO algorithm for automatic generation control of linear and nonlinear interconnected power systems", *Appl Soft Comput.*13. 4718–4730, 2013.
- [6] RK. Sahu, S. Panda, G.T.C. Sekhar, "A novel hybrid PSO-PS optimized fuzzy PI controller for AGC in multi area interconnected power systems", *International Journal of Electrical Power & Energy Systems*, 2015, 64, pp.880-893.
- [7] Y. Arya, "Improvement in automatic generation control of two- area electric power systems via a fuzzy aided optimal PIDN- FOI controller," *ISA transactions*, 2018, 80, pp. 475-490.
- [8] Y. Arya, Kumar, "BFOA-scaled fractional order fuzzy PID controller applied to AGC of multi-area multi-source electric power generating systems", *Swarm and Evolutionary Computation*, 2017, 32, pp. 202-218.
- [9] PS. Mishra, R.C. Prusty, S. Panda, "Improved-salp swarm optimized type-II fuzzy controller in load

- frequency control of multi area islanded AC microgrid, Sustainable Energy", Grids and Networks. 16 (2018) 380-392.
- [10] A. Fereidouni, A. S. Masoum, M. Moghbel, "A new adaptive configuration of PID type fuzzy logic controller", ISA Trans. 56 (2015) 222-240.
- [11] B. Mohanty, S.Panda. and PK. Hota, "Controller parameters tuning of differential evolution algorithm and its application to load frequency control of multi-source power system", Electrical Power and Energy Systems, Vol. 54, pp. 77-85,2014.
- [12] RK. Sahu, S.Panda and UK. Rout, "DE optimized parallel 2-DOF PID controller for load frequency control of power system with governor dead-band nonlinearity", Electrical Power and Energy Systems, Vol. 49, pp. 19-33,2013.
- [13] PC. Nayak, A. Sahoo, R. Balabantaray, RC. Prusty, "Comparative study of SOS & PSO for fuzzy based PID controller in AGC in an integrated power system", IEEE conference on Technologies for Smart – City Energy Security and Power, Vol. 1, pp.1-6,2018.
- [14] S. Panda, B. Mohanty, and PK. Hota, "Hybrid BFOA-PSO algorithm for automatic generation control of linear and nonlinear interconnected power systems", Applied Soft Computing, Vol. 13No. 12, pp. 4718-4730,2013.
- [15] K. Naidu, H. Mokhlis, and AH. Bakar, "Multi-objective optimization using weighted sum Artificial Bee Colony algorithm for load frequency control", Electrical Power and Energy Systems, Vol. 55, pp. 657-667,2014.
- [16] P. Dash, LC. Saikia and N. Sinha, "Comparison of performance of several cuckoo search algorithm based 2DOF controllers in AGC of multi-area thermal system", Electrical Power and Energy Systems, Vol. 55, pp. 429-436,2014.
- [17] AK. Barisal, "Comparative performance analysis of teaching learning-based optimization for automatic load frequency control of multi-source power systems", Electrical Power and Energy Systems, Vol. 66, pp. 66-77,2015.
- [18] SR. Khuntia and S.Panda, "Simulation study for automatic generation control of a multi-area power system by ANFIS approach", Applied Soft Computing, Vol. 12, pp. 333-341,2012.
- [19] P. Dash, LC. Saikia, and N. Sinha, "Automatic generation control of multi area thermal system using bat algorithm optimized PD–PID Cascade controller", Electrical Power and Energy Systems, Vol. 68, pp. 364-372,2015.
- [20] S.Padhy, S.Panda, and Mahapatra, "A modified GWO technique-based cascade PI-PD controller for AGC of power systems in presence of plug in Electric vehicles", Engineering Science and Technology, Vol. 20 No. 2, pp. 427-442,2017.
- [21] PC. Sahu, RC. Prusty and S.Panda, "A gray wolf optimized FPD plus (1+PI) multistage controller for AGC of multisource non-linear power system", World Journal of Engineering,2019.
- [22] Gomes, G. F., da Cunha, S. S. & Ancelotti, A. C., A sunflower optimization (SFO) algorithm applied to damage identification on laminated composite plates. Engineering with Computers, Volume 35, p. 619–626,2018.
- [23] D.L. Lee, L. Wang," Small-signal stability analysis of an autonomous hybrid renewable energy power generation/energy storage system part I: Time-domain simulations", IEEE Transactions on energy conversion, 2008 (23), pp.311-320.
- [24] K. Singh, M. Amir, F. Ahmad, MA. Khan, "An Integral Tilt Derivative Control Strategy for Frequency Control in Multi-microgrid System", IEEE Systems Journal, 2020.
- [25] PC. Nayak, S. Mishra, RC. Prusty & S. Panda, "Performance analysis of hydrogen aqua equalizer fuel-cell on AGC of Wind-hydro-thermal power systems with sunflower algorithm optimized fuzzy-PDFPI controller", International Journal of Ambient Energy, Volume 43, pp. 1-14,2020.
- [26] NK. Jena, NC.Patel, S.Sahoo, BK. Sahu, SS.Dash, R.Bayindir, "Application of fractional order cascaded controller for AGC study in power system integrated with renewable sources", International Journal of Renewable Energy Research (IJRER). 2020 Mar 25;10(1):89-100.
- [27] PC. Babu, SS. Dash, R. Bayindir, RK. Behera, CH. Subramani, "Analysis and experimental investigation for grid-connected 10 kW solar PV system in distribution networks", IEEE International Conference on Renewable Energy Research and Applications (ICRERA) 2016 Nov 20 (pp. 772-777). IEEE.
- [28] KS. Rajesh, SS. Dash, R. Sridhar, R. Rajagopal, "Implementation of an adaptive control strategy for solar photo voltaic generators in microgrids with MPPT and energy storage", IEEE International Conference on Renewable Energy Research and Applications (ICRERA) 2016 Nov 20 (pp. 766-771). IEEE.
- [29] G. Todeschini, H. Huang, N. Bristow, TW. David, J. Kettle, "A Novel Computational Model for Organic PV Cells and Modules", International Journal of Smart Grid-ijSmartGrid. 2020 Dec 22;4(4):157-63.
- [30] NK. Kasim, HH. Hussain, AN. Abed, "Performance analysis of grid-connected CIGS PV solar system and comparison with PVsyst simulation program", International Journal of Smart Grid. 2019; 3:172-9.
- [31] A. Belkaid, I. Colak, K. Kayisli, M. Sara, R. Bayindir, "Modelling and simulation of polycrystalline silicon photovoltaic cells", 7th IEEE International Conference on Smart Grid (icSmartGrid) 2019 Dec 9 (pp. 155-158).